

## Nonvolatile Si Si O 2 Si N Si O 2 Si type polycrystalline silicon thin-film-transistor memory with nanowire channels for improvement of erasing characteristics

Shih-Ching Chen, Ting-Chang Chang, Po-Tsun Liu, Yung-Chun Wu, Jing-Yi Chin, Ping-Hung Yeh, Li-Wei Feng, S. M. Sze, Chun-Yen Chang, and Chen-Hsin Lien

Citation: *Applied Physics Letters* **91**, 193103 (2007); doi: 10.1063/1.2798600

View online: <http://dx.doi.org/10.1063/1.2798600>

View Table of Contents: <http://scitation.aip.org/content/aip/journal/apl/91/19?ver=pdfcov>

Published by the [AIP Publishing](#)

---

### Articles you may be interested in

Impact of interface controlling layer of Al 2 O 3 for improving the retention behaviors of In–Ga–Zn oxide-based ferroelectric memory transistor

*Appl. Phys. Lett.* **96**, 232903 (2010); 10.1063/1.3452339

Organic floating-gate transistor memory based on the structure of pentacene/nanoparticle- Al / Al 2 O 3

*Appl. Phys. Lett.* **96**, 203304 (2010); 10.1063/1.3432667

Ti Si 2 Si heteronanocrystal metal-oxide-semiconductor-field-effect-transistor memory

*Appl. Phys. Lett.* **89**, 233113 (2006); 10.1063/1.2402232

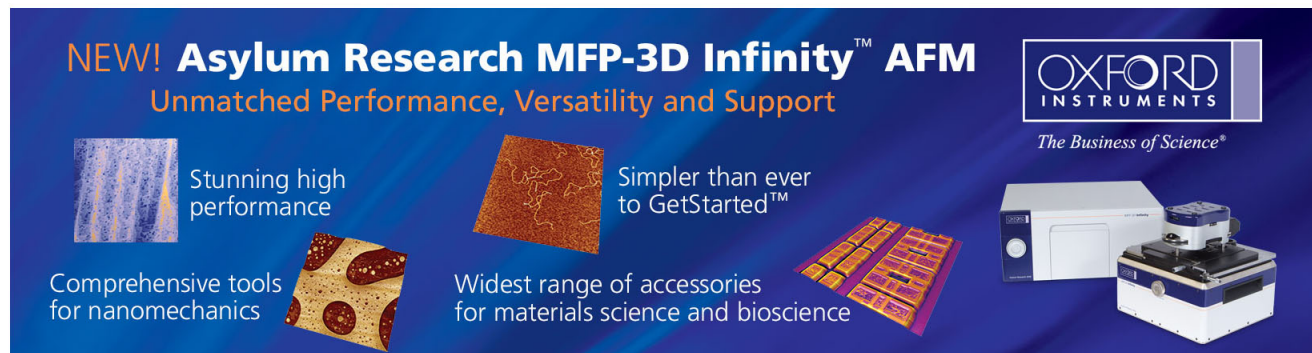
Visualization of electrons and holes localized in gate thin film of metal Si O 2 – Si 3 N 4 – Si O 2 semiconductor-type flash memory using scanning nonlinear dielectric microscopy after writing-erasing cycling

*Appl. Phys. Lett.* **86**, 063515 (2005); 10.1063/1.1862333

Polycrystalline silicon/CoSi 2 Schottky diode with integrated SiO 2 antifuse: a nonvolatile memory cell

*Appl. Phys. Lett.* **82**, 4163 (2003); 10.1063/1.1581364

---

The advertisement features a dark blue background with white and orange text. At the top left, it says 'NEW! Asylum Research MFP-3D Infinity™ AFM' in large white letters, followed by 'Unmatched Performance, Versatility and Support' in orange. On the right, the Oxford Instruments logo is shown with the tagline 'The Business of Science®'. Below the text are four images: a blue textured surface, a brown textured surface, a grid of yellow and red squares, and a photograph of the AFM instrument. Text descriptions are placed around these images: 'Stunning high performance' next to the blue surface, 'Simpler than ever to GetStarted™' next to the brown surface, 'Comprehensive tools for nanomechanics' next to the grid, and 'Widest range of accessories for materials science and bioscience' next to the instrument photo.

## Nonvolatile Si/SiO<sub>2</sub>/SiN/SiO<sub>2</sub>/Si type polycrystalline silicon thin-film-transistor memory with nanowire channels for improvement of erasing characteristics

Shih-Ching Chen

*Department of Physics, National Sun Yat-Sen University, Kaohsiung 804, Taiwan, Republic of China*

Ting-Chang Chang<sup>a)</sup>

*Department of Physics and Institute of Electro-Optical Engineering, Center for Nanoscience and Nanotechnology, National Sun Yat-Sen University, Kaohsiung 804, Taiwan, Republic of China*

Po-Tsun Liu

*Department of Photonics and Display Institute, National Chiao Tung University, Hsin-Chu 300, Taiwan, Republic of China*

Yung-Chun Wu

*Department of Engineering and System Science, National Tsing-Hua University, Hsin-Chu 300, Taiwan, Republic of China*

Jing-Yi Chin

*Department of Physics, National Sun Yat-Sen University, 70 Lien-hai Rd., Kaohsiung 804, Taiwan, Republic of China*

Ping-Hung Yeh

*Department of Materials Science and Engineering, National Tsing Hua University, Hsin-Chu 300, Taiwan, Republic of China*

Li-Wei Feng, S. M. Sze, and Chun-Yen Chang

*Institute of Electronics, National Chiao Tung University, Taiwan, Hsin-Chu 300, Taiwan, Republic of China*

Chen-Hsin Lien

*Institute of Electronics Engineering, National Tsing Hua University, Hsin-Chu 300, Taiwan, Republic of China*

(Received 12 July 2007; accepted 24 September 2007; published online 5 November 2007)

A silicon-oxide-nitride-oxide-silicon type polycrystalline silicon thin-film transistor (poly-Si TFT) with nanowire channels was investigated for both transistor and memory applications. The poly-Si TFT memory device has superior electrical characteristics, such as higher drain current, smaller threshold voltage, and steeper subthreshold slope. Also, the simulation result on electrical field reveals that the electrical field across the tunnel oxide is enhanced and that across the blocking oxide is reduced at the corner regions. This will lead to the parasitic gate injection activity and the erasing speed can be apparently improved in the memory device due to the pronounced corner effect and narrow channel width. © 2007 American Institute of Physics. [DOI: 10.1063/1.2798600]

System-on-panel (SOP) display technology with high performance polycrystalline silicon thin-film transistors (poly-Si TFTs) designed as functional devices has rapidly advanced recently.<sup>1,2</sup> The SOP technology primarily focuses on mobile electronics application; thus, low power consumption is required for a long battery life. It is well known that the nonvolatile memory is widely utilized for data storage in portable electronics system due to its properties of low-power consumption and nonvolatility. Compared to conventional nonvolatile memory with floating gate structure, the silicon-oxide-nitride-oxide-silicon (SONOS) type poly-Si TFT memory devices have been proposed for SOP application due to its full process compatibility.<sup>3</sup> A SONOS memory array using Fowler-Nordheim (FN) tunneling for program/erase ( $P/E$ ) operation has been demonstrated to achieve the low power consumption requirement compared with channel

hot electron injection scheme.<sup>4</sup> However, this type of SONOS memory still has several issues on performance, such as insufficient programing/erasing ( $P/E$ ) efficiency and an undesirable gate injection phenomenon.<sup>5</sup> Recently, various approaches have been proposed to improve the  $P/E$  speed and gate injection by using high- $k$  dielectric as a blocking layer.<sup>6,7</sup> The electric field in high- $k$  dielectric is lower than that in the typical SiO<sub>2</sub> film, and thus, it is expected that parasitic gate injection through blocking oxide should be suppressed. In addition, gate engineering methods also proposed by using high work function materials<sup>8,9</sup> to reduce the unwanted charge transport from gate. In this paper, the poly-Si TFT combined with nonvolatile SONOS memory and nanowire channels, called NW SONOS-TFT, is proposed. Not only does the NW device exhibit superior electrical performance for transistor, but it can also suppress the undesirable gate injection and improve the erasing speed for the memory device. The most important is that the fabrication involves no materials replacement, and thereby it is very promising for SOP application in the future.

<sup>a)</sup> Author to whom correspondence should be addressed. Tel.: 886-7-5252000 ext. 7710. FAX: 886-7-5253709. Electronic mail: techang@mail.phys.nsysu.edu.tw

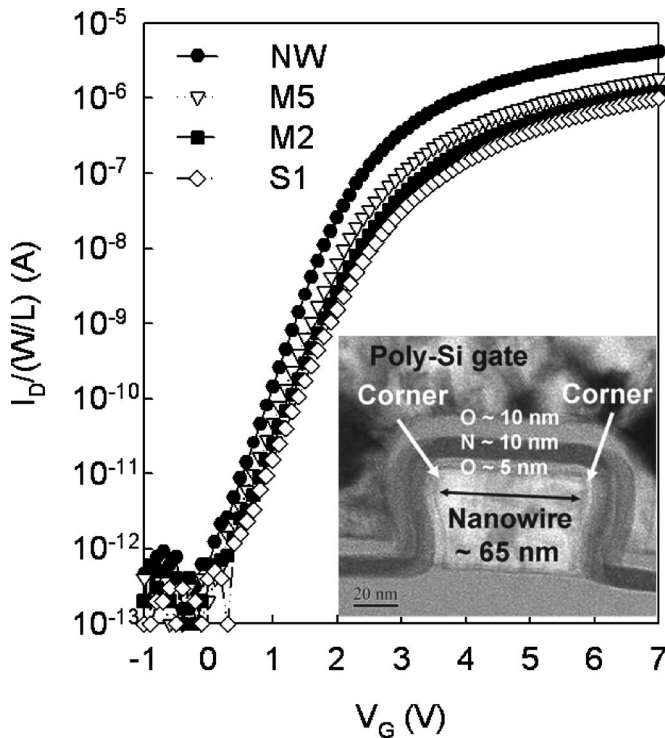


FIG. 1. Comparison of typical  $I_D$ - $V_G$  characteristics of the SONOS-TFTs with various structures. The inset exhibits the transmission electron microscopy (TEM) of a single nanowire channel of NW SONOS-TFT.

A 400-nm-thick thermal oxide layer was first grown on the Si wafer by furnace system to replace a glass substrate. Then an undoped 50-nm-thick amorphous silicon (*a*-Si) layer was deposited on the oxidized silicon wafer by low-pressure chemical vapor deposition (LPCVD) at 550 °C. Subsequently, the deposited *a*-Si layer was recrystallized by solid-phase crystallization at 600 °C for 24 h under  $N_2$  ambient. After the patterning of active region with electron beam lithography and dry etching process, the 25-nm-thick oxide-nitride-oxide (ONO) multilayer gate dielectric layers were formed by LPCVD: the 5 nm tunnel oxide (TO), 10 nm silicon nitride (SiN), and 10 nm blocking oxide (BO), sequentially. A 150-nm-thick *in situ*  $n^+$  doped poly-Si layer was then deposited and defined. After *S/D* formation by self-aligned phosphorous implantation, a 200 nm oxide passivation layer was deposited and contact holes were patterned. Finally, Al metallization was performed and the devices were sintered at 400 °C in nitrogen ambient for 30 min. The studied TFT devices with the same gate length of 5  $\mu\text{m}$  consist of different channels in width, including ten strips of 65 nm nanowire (NW), five strips of 200 nm channels (M5), two strips of 500 nm channels (M2), and a single-channel (S1) with 1  $\mu\text{m}$ .

Figure 1 presents the transfer normalized  $I_D$ - $V_G$  curves of SONOS-TFTs with various structures. Obviously, the NW device has superior performance, such as the highest drain current, smallest threshold voltage ( $V_{th}$ ), and steepest subthreshold swing (SS). The  $V_{th}$  decreases from 2.5 V to 1.7 V and SS decreases from 0.5 to 0.4 V/decade in order from the S1 structure to the NW structure. Different from the other structures, the nanowire is surrounded by the poly-Si gate to form the trigate structure, shown as the inset TEM photograph. The physical width of nanowire channel is confirmed to be 65 nm and the thickness of ONO is 25 nm. Since the

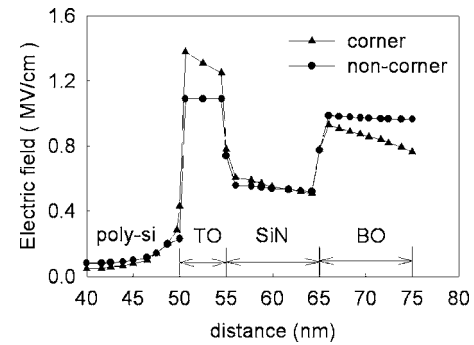


FIG. 2. Simulation of the electrical fields with a gate bias of 2 V in nanowire at corner and noncorner regions.

effective channel width is increased by the trigate structure, the drain current can be improved in NW SONOS-TFT. To study the electrical improvement for the subthreshold behavior, the distribution of electrical field across the stacked gate dielectric of nanowire channel were numerically simulated at a gate bias of 2 V ( $\sim V_{th}$ ) by ISE-TCAD simulator, as shown in Fig. 2. It can be seen that the electrical field near the  $\text{SiO}_2$ /poly-Si interface at corner region is very high. This will lead the current at the corner region to turn on earlier than that at the noncorner region due to the corner effect induced electrical field. The corner current can provide major current as the device operated in subthreshold region.<sup>10</sup> Thus, the corner effect plays a dominant role to enhance the subthreshold behavior.

The SONOS-TFTs also can act as a nonvolatile memory by using the nitride layer as a charge trapping layer, in addition to transistor application. Figure 3 shows the  $I_D$ - $V_G$  curves of device before and after the programming/erasing operations by FN tunneling scheme. The results reveal that the threshold voltage of a fresh memory device is different from those of the memory device after erasing operation. Because the electrons will inject to silicon nitride layer from the control gate via FN tunneling, it is difficult for the SONOS-TFT memory to return to the original state of threshold voltage after performing an erase procedure.

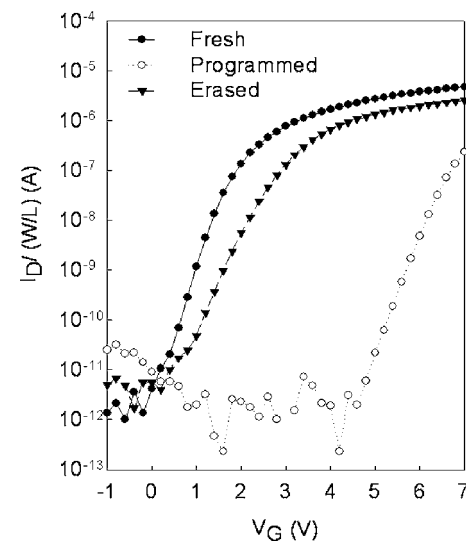


FIG. 3. The  $I_D$ - $V_G$  curves of device before memory operation (fresh) and after the programming/erasing operations. The program and erase conditions are 16 V for 100  $\mu\text{s}$  and -18 V for 10 s, respectively.

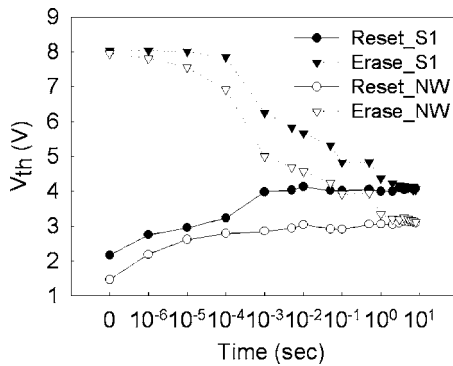


FIG. 4. Self-convergent reset-erase characteristics of S1 and NW devices with a  $-18$  V erasing bias. The devices are both programmed with a  $18$  V gate bias.

Figure 4 presents the self-convergent reset-erase characteristics of the S1 and NW devices. Firstly, the fresh devices were reset by FN mechanism erase with a  $-18$  V to achieve the dynamic balance condition. Next, the devices were programmed and then erased with the same negative bias. The results reveal that the self-convergent property is really caused by the balance of electron injection from gate and electron detrapping to substrate. Thus, the reset state  $V_{th}$  is determined by the dynamic current balance through the ONO layer. It can be found that the NW device has a smaller reset voltage than that of S1 device. Moreover, the erasing speed is also enhanced in NW structure. Figure 5 shows the threshold voltage shift ( $V_{th,reset} - V_{th,fresh}$ ) before and after the memory operation with various structures. Obviously, the  $V_{th}$  shift is almost the same for S1 and M2 devices, and then it decreases as the channel width decreases and corner numbers

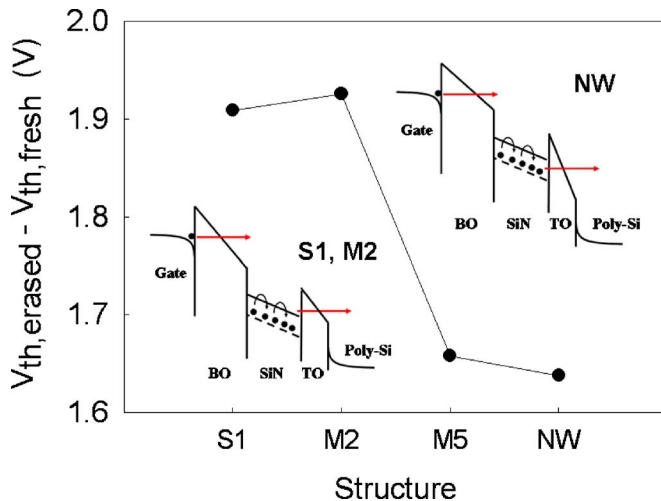


FIG. 5. Threshold voltage shift ( $V_{th,reset} - V_{th,fresh}$ ) vs different structures. The insets exhibit the schematic band diagrams at corner (for NW structure) and noncorner (for S1, M2 structures) regions.

increase. Due to the pronounced corner effect and narrow channel width, the memory characteristic is dominated by the electrons stored in nitride layer at the corner regions for NW device. Comparing the electrical fields at noncorner region, the electrical field across the tunnel oxide is greatly enhanced and the electric field across the blocking oxide is slightly reduced. The schematic band diagrams across ONO layer are illustrated in the inset. Therefore, the parasitic gate injection and the erasing speed can be improved for NW device due to the corner effect.

In conclusion, we have demonstrated the SONOS type poly-Si TFT memory with nanowire channels. Since the effective channel width is increased by trigate structure and the subthreshold behavior is improved by additional corner current, the NW device has superior transistor performance than other devices. As the devices operated for memory mode by using FN tunneling mechanism, the self-convergent characteristics reveal the undesirable gate injection and inefficient erase speed can be improved apparently from S1 to NW structure. According to the simulated results, the improvement for the transistor and memory with nanowire structure is mainly contributed to the pronounced corner effect. Although the NW devices cannot be easily fabricated using panel maker's existing manufacturing facilities at present time, it is still a very promising technology because of no material replacement.

This work was performed at National Nano Device Laboratory and was supported by the National Science Council of the Republic of China under Contract Nos. NSC-96-2120-M-110-001 and 95-2221-E-009-316-MY2. Also, this work was partially supported by MOEA Technology Development for Academia Project.

<sup>1</sup>K. Yoneda, R. Yokoyama, and T. Yamada, in Proc. Symp. VLSI Circuits, 2001, pp. 85–90.

<sup>2</sup>T. Nishibe and H. Nakamura, in Proc. SID, 2006, pp. 1091–1094.

<sup>3</sup>Y. H. Lin, C. H. Chien, T. H. Chou, T. S. Chao, and T. F. Lei, IEEE Trans. Electron Devices **54**, 531 (2007).

<sup>4</sup>A. Nakamura, H. Moriya, T. Terano, H. Kosaka, A. Hashiguchi, K. Nomoto, I. Fujiwara, T. Kobayashi, and T. Oda, IEEE Trans. Electron Devices **51**, 895 (2004).

<sup>5</sup>H. T. Lue, Y. H. Shih, K. Y. Hsieh, R. Liu, and C. Y. Lu, IEEE Electron Device Lett. **25**, 816 (2004).

<sup>6</sup>X. Wang and D. L. Kwong, IEEE Trans. Electron Devices **53**, 78 (2006).

<sup>7</sup>V. A. Gritsenko, K. A. Nasyrov, Y. N. Novikov, A. L. Aseev, S. Y. Yoon, J. W. Lee, E. H. Lee, and C. W. Kim, Solid-State Electron. **47**, 1651 (2003).

<sup>8</sup>C. Friederich, M. Specht, T. Lutz, F. Hofmann, L. Dreeskornfeld, W. Weber, J. Kretz, T. Melde, W. Rosner, E. Landgraf, J. Hartwich, M. Stadelé, L. Risch, and D. Richter, Tech. Dig. - Int. Electron Devices Meet. **2006**, 346946.

<sup>9</sup>C. H. Lee, K. C. Park, and K. Kim, Appl. Phys. Lett. **87**, 073510 (2005).

<sup>10</sup>B. Doyle, B. Boyanov, S. Datta, M. Doczy, S. Harelend, B. Jin, J. Kavalieros, T. Linton, R. Rios, and R. Chau, in Proc. VLSI Tech. Symp., 2003, pp. 133–134.